Formation of Lithiated Adducts of Glycerophosphocholine Lipids Facilitates their Identification by Electrospray Ionization Tandem Mass Spectrometry

Fong-Fu Hsu, Alan Bohrer, and John Turk

Mass Spectrometry Resource, Division of Diabetes, Endocrinology and Metabolism, Department of Medicine, Washington University School of Medicine, St. Louis, Missouri, USA

Electrospray ionization (ESI) tandem mass spectrometry (MS) has simplified analysis of phospholipid mixtures, and, in negative ion mode, permits structural identification of picomole amounts of phospholipid species. Collisionally activated dissociation (CAD) of phospholipid anions yields negative ion tandem mass spectra that contain fragment ions representing the fatty acid substituents as carboxylate anions. Glycerophosphocholine (GPC) lipids contain a quaternary nitrogen moiety and more readily form cationic adducts than anionic species, and positive ion tandem mass spectra of protonated GPC species contain no abundant ions that identify fatty acid substituents. We report here that lithiated adducts of GPC species are readily formed by adding lithium hydroxide to the solution in which phospholipid mixtures are infused into the ESI source. CAD of [MLi^+] ions of GPC species yields tandem mass spectra that contain prominent ions representing losses of the fatty acid substituents. These ions and their relative abundances can be used to assign the identities and positions of the fatty acid substituents of GPC species. Tandem mass spectrometric scans monitoring neutral losses of the head-group or of fatty acid substituents from lithiated adducts can be used to identify GPC species in tissue phospholipid mixtures. Similar scans monitoring parents of specific product ions can also be used to identify the fatty acid substituents of GPC species, and this facilitates identification of distinct isobaric contributors to ions observed in the ESI/MS total ion current. (J Am Soc Mass Spectrom 1998, 9, 516–526) © 1998 American Society for Mass Spectrometry

Phospholipids are essential components of cellular membranes [1], and distinct molecular species are differentially distributed among tissues and within subcellular compartments [2–5]. The phospholipid composition of cell membranes influences their fusion with other membrane compartments [6, 7] and cell growth and death [8]. Hydrolysis of phospholipid molecules to yield second messenger substances is involved in transduction of signals from the extracellular to the intracellular environment [9–14], and transfer of fatty acid moieties among phospholipid classes is complex and regulated [8, 15–17]. Sensitive analytical methods to identify components of phospholipid mixtures may facilitate the study of processes governing the distribution of distinct phospholipid molecular species at biologic loci, particularly with membranes obtainable only in small quantities from specialized cells or intracellular compartments [4, 5].

Glycerophospholipids contain a glycerol backbone, and, in the sn-3 position, bear a phosphodiester moiety linked to a polar head-group, such as choline, ethanolamine, serine, inositol, or glycerol [18]. Fatty acid moieties are esterified to the sn-2 and often the sn-1 positions of the glycerol backbone, although ether linkages to fatty alcohol or aldehyde residues may also occur in the sn-1 position [18]. Fatty acid residues of various chain lengths and degrees of unsaturation may be distributed symmetrically or asymmetrically in the sn-1 and sn-2 positions, resulting in complex biological phospholipid mixtures. Conventional methods for determining identities and abundances of components of phospholipid mixtures involve multiple steps [4, 5, 15, 19]. One approach involves normal phase high performance liquid chromatography (HPLC) analysis to separate phospholipid head-group classes and then reverse phase HPLC analysis to separate molecular species [19]. Each isolated species is subjected to solvolysis to yield products from fatty acid, alcohol, or aldehyde moieties, and these components are derivatized and analyzed by gas chromatography/mass spectrometry (GC/MS) [4, 5, 15]. This complex procedure may result in analyte losses during each processing step and in ambiguous

Address reprint requests to Dr. John Turk, Department of Medicine, Box 8127, Washington University School of Medicine, 660 South Euclid Avenue, St. Louis, MO 63110.

1044-0305/98/$19.00
PII S1044-0305(98)00012-9

Received September 3, 1997
Revised November 13, 1997
Accepted December 30, 1997

assignments when HPLC separation of molecular species is incomplete.

Fast atom bombardment (FAB)/MS permits direct analysis of phospholipids as intact molecules [18, 20–25], thereby circumventing solvolysis and derivatization. When combined with collisionally activated dissociation (CAD) and tandem mass spectrometry, FAB permits direct identification of phospholipid molecular species [18]. The sensitivity of FAB/MS is limited by matrix-derived background ions, and this precludes its application to some biological phospholipid mixtures obtainable in only small quantities [4, 5]. Electrospray ionization (ESI) offers greater sensitivity than FAB for phospholipid analysis, and ESI/MS/MS permits identification of picomole quantities of phospholipid species in biological mixtures [26–29].

The tandem mass spectra produced by CAD of phospholipid ions are similar when ionization is achieved by FAB or by ESI [18, 27]. Glycerophospholipid species which contain head-groups (e.g., ethanolamine, serine, inositol, or glycerol) that readily form anions yield negative ion tandem mass spectra that identify the fatty acid substituents [18, 27]. Each substituent is represented by its carboxylate anion, and the relative abundances of these ions reflect the positions of the substituents [18, 27]. Glycerophosphocholine (GPC) species are the most abundant constituents of mammalian cell membranes, contain a quaternary nitrogen with a fixed positive charge, and more readily form positive than negative ions. Positive ion tandem mass spectra of protonated adducts of GPC species are dominated by phosphocholine ion and contain no abundant ions that identify the fatty acid substituents [18, 27].

In FAB, negative ions are formed from GPC species by loss of methyl substituents from the quaternary nitrogen, loss of trimethylamine, and loss of the choline moiety [18, 30]. CAD of these ions yields tandem mass spectra that permit assignments of the identities and positions of fatty acid substituents [18, 30]. The modest intensity of such ions in negative ion ESI/MS analyses of GPC species has caused examination of chloride adducts of GPC species, and CAD of $[MCl^-]$ ions yields tandem mass spectra that contain carboxylate anions of the fatty acid substituents [28]. The $[^{35}Cl]/[^{37}Cl]$ isotopic distribution complicates interpretation of ESI/MS surveys of components of tissue GPC mixtures because the molecular weights of individual GPC species may differ by 2 u, owing to a difference of a single degree of carbon–carbon unsaturation in the fatty acid substituents. Analysis of GPC species by continuous flow liquid secondary ion mass spectrometry in negative ion mode has also been reported to yield less signal than analysis of cationic adducts in positive ion mode [31].

We report here that lithiated adducts of GPC species can be readily analyzed by positive ion ESI/MS, and that CAD of these adducts yields tandem mass spectra that contain ions reflecting the identities and positions of the fatty acid substituents.

Materials and Methods

Materials

Standard GPC species with defined fatty acid substiutents were obtained from Avanti Polar Lipids (Birmingham, AL). Solvents were obtained from Burdick and Jackson (Muskegee, MI). Lithium salts were obtained from Sigma Chemical Co. (St. Louis, MO). Male Sprague Dawley rats were obtained from Harlan (Indianapolis, IN) and fed with Rodent Chow 5001 (Ralston Purina, St. Louis, MO).

Preparation of Tissue Phospholipid Extracts

Male Sprague-Dawley rats (200–250 g body weight) were anesthetized by intraperitoneal injection of sodium pentobarbital (45 mg/kg). When corneal reflexes were absent, the abdomen was incised and the liver removed and placed in ice-cold phosphate-buffered saline (PBS). The top of the cranium was removed and the brain excised and placed in ice-cold PBS. Tissue samples were rinsed twice in ice-cold PBS and minced. Minced tissue (1 g wet weight) was suspended in a solution (2 mL) of chloroform/methanol (1/1, v/v) and homogenized with a Tissue-Tearor (setting 7, 1 min, Biospec Products, Bartlesville, OK). Homogenates were sonicated on ice with a Vibra Cell probe sonicator apparatus (20% power, 5 s bursts, 1 min, Sonics and Materials, Danbury, CT). Samples were centrifuged (2800 $\times$ g, 5 min) to remove tissue debris. Supernatants were transferred to silanized glass tubes and extracted [32] by adding methanol (1 mL), chloroform (1 mL), and water (1.8 mL). Samples were vortex mixed and centrifuged (900 $\times$ g, 5 min). Supernatants were removed, concentrated to dryness under nitrogen, and reconstituted as specified below.

Mass Spectrometry

ESI/MS analyses were performed on a Finnigan (San Jose, CA) TSQ-7000 triple stage quadrupole spectrometer equipped with an ESI source and controlled by Finnigan ICIS software operated on a DEC alpha workstation. Solutions of standard phospholipids or tissue extracts were dissolved in methanol/chloroform (90/10) at final concentrations of about 1 pmol/μL. To form lithiated adducts of GPC species, LiOH (2 nmol/μL final concentration) was added to this solution. Samples were infused (1 μL/min) into the ESI source with a Harvard syringe pump. The electrospray needle and the skimmer were at ground potential and the electrospray chamber and the entrance of the glass capillary at 4.4 kV. The heated capillary temperature was 250°C. For collisionally activated dissociation (CAD) and tandem mass spectrometry, the collision gas was argon (2.2–2.5 mtorr), and collision energies were varied between 32 and 36 eV. Product ion spectra were acquired using a signal-averaging protocol in profile mode at a rate of 1

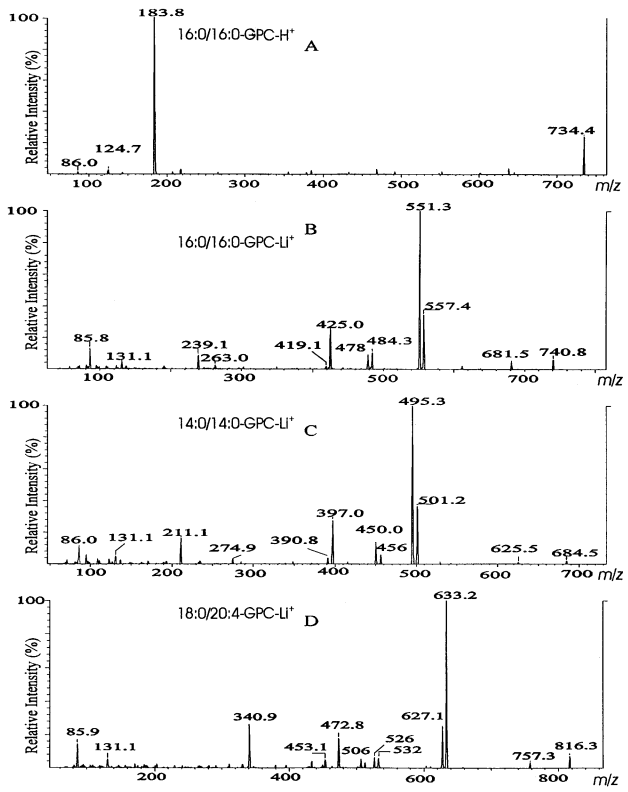

Figure 1. Positive ion ESI tandem mass spectra of cationic adducts of standard glycerophosphocholine species. Panels are tandem mass spectra obtained from CAD of the [MH^+] ion of dipalmitoyl-GPC (panel A), the [MLi^+] ion of dipalmitoyl-GPC (panel B), the [MLi^+] ion of dimyristoyl-GPC (panel C), or the [MLi^+] ion of (1-stearoyl, 2-arachidonoyl)-GPC (panel D).

scan per 3 s. In some cases, neutral loss scans were performed to identify parent ions that yielded product ions that had undergone losses of 59, 183, or 189 from the mass-to-charge ratio value of the parent ion. In other cases, parent ions were identified that yielded product ions of a specific mass-to-charge ratio value, e.g., m/z 397, 425, 453, 451, 449, 473, or 497. It was found that lithiated adducts of GPC species could also be formed by adding lithium acetate, lithium chloride, or lithium fluoride to the infusion solution. With lithium acetate, [MLi^++66] ions were observed in addition to [MLi^+] ions. Tandem mass spectra of [MLi^++66] ions indicated that they represented lithium acetate adducts of [MLi^+] ions. These adduct ions constituted up to 30% of the total ion current. With lithium chloride and lithium fluoride, [MH^+] ions were observed in addition to [MLi^+] ions.

Results

The positive ion ESI/MS/MS spectra of cationic adducts of synthetic standard GPC species containing symmetrical sn-1 and sn-2 fatty acid substituents were determined first. As illustrated in Figure 1A, the CAD of the [MH^+] ion (m/z 734) of dipalmitoyl-GPC [(16:0/16:0)-GPC] yields a tandem mass spectrum dominated by an ion at m/z 184 ([$H_2PO_4(CH_2)_2N(CH_3)_3]^+$). This spectrum contains no abundant ions that identify fatty acid substituents, concordant with previous reports on the tandem mass spectra of protonated GPC species generated by FAB or ESI [18, 20–23, 27]. In contrast, the lithiated adduct of (16:0/16:0)-GPC exhibits a more complex fragmentation pattern upon CAD (Figure 1B). CAD of the [MLi^+] ion (m/z 740) results in neutral loss of trimethylamine ($MLi^+ - 59$) to yield an ion at m/z 681. Ions at m/z 557 ($MLi^+ - 183$) and m/z 551 ($MLi^+ - 189$) are presumed to reflect net, though probably not direct, loss of [$HPO_4(CH_2)_2N(CH_3)_3$] or of [$LiPO_4(CH_2)_2N(CH_3)_3$], respectively. Subsequent spectra indicate that losses of 59, 183, and 189 are common to the tandem spectra of all GPC-Li^+ species, regardless of the nature of the fatty acid substituents, and the possible genesis of these losses is discussed further below. Ions resulting from these losses reflect the phosphocholine head-group but do not yield information about fatty acid substituents.

The CAD spectrum of (16:0/16:0)-GPC-Li^+ (Figure 1B) also contains ions at m/z 484, m/z 478, and m/z 425 (Figure 1B), which may reflect neutral losses of palmitic acid (MLi − 256), of the lithium salt of palmitate (MLi − 262), and of trimethylamine plus palmitic acid (MLi − 315), respectively. In addition, an ion at m/z 239 may represent the acylium ion derived from palmitate. These assignments are supported by the tandem spectrum obtained by CAD of the [MLi^+] ion (m/z 684) of dimyristoyl-GPC [(14:0/14:0)-GPC] (Figure 1C). This spectrum contains ions at m/z 456, m/z 450, and m/z 397, which are consistent with neutral loss of myristic acid (MLi − 228), of the lithium salt of myristate (MLi − 234), and of trimethylamine plus myristic acid (MLi − 287), respectively. The acylium ion (m/z 211) derived from myristate is also observed (Figure 1C).

The behavior of a standard GPC species with asymmetrical fatty acid substituents was examined next. CAD of the [MLi^+] ion (m/z 816) of (1-stearoyl, 2-arachidonoyl)-GPC [(18:0/20:4)-GPC] yields a tandem mass spectrum (Figure 1D) which contains ions consistent with neutral losses of trimethylamine plus either the sn-1 fatty acid substituent ($MLi^+ - 343$) or the sn-2 substituent ($MLi^+ - 363$) as free fatty acids at m/z 473 and m/z 453, respectively. The former ion is more abundant than the latter, suggesting that the relative abundance of ions reflecting these losses may indicate the positions of the fatty acid substituents, as discussed further below. Figure 1D also illustrates that neutral losses of the sn-1 fatty acid substituent as a free fatty acid ($MLi^+ - 284$) or as a lithium salt ($MLi^+ - 290$) are also observed at m/z 532 and m/z 526, respectively. In addition, neutral losses of the sn-2 fatty acid substituent as a free fatty acid ($MLi^+ - 304$) or as a lithium salt ($MLi^+ - 310$) are observed at m/z 512 and m/z 506, respectively.

A prominent ion (m/z 341, $MLi^+ - 475$) in the tandem spectrum (Figure 1D) of (18:0/20:4)-GPC-Li^+ is

consistent with net, though probably not direct, elimination of $[LiPO_4(CH_2)_2N(CH_3)_3]$ and loss of the sn-2 substituent as a substituted ketene. An analogous and similarly prominent ($MLi^+ - 475$) ion is observed in the tandem mass spectrum of the lithiated adduct of standard (1-palmitoyl, 2-arachidonoyl)-GPC [(16:0/20:4)-GPC] (not shown). No analogous ions of comparable abundance are observed in the tandem spectra of GPC species, which contain sn-2 substituents with less than three carbon–carbon double bonds, suggesting that net elimination of $[LiPO_4(CH_2)_2N(CH_3)_3]$ and the sn-2 substituent as a ketene requires a polyunsaturated sn-2 substituent. No prominent acylium ions are observed in the tandem spectrum of (18:0/20:4)-GPC-Li^+ (Figure 1D), and subsequent spectra suggest that acylium ions may be formed preferentially with saturated sn-2 fatty acid substituents and less readily with sn-1 substituents or with unsaturated fatty acids.

The two most abundant ions in the spectra in Figure 1B, C, D are $[MLi^+ - 189]$ and $[MLi^+ - 183]$. Formation of these ions may involve initial loss of trimethylamine and formation of an intermediate structure containing a five-membered cyclophosphane moiety, as illustrated in Figure 2. The cyclophosphane moiety may then be eliminated as a neutral lithium salt to yield the $[MLi^+ - 189]$ ion depicted in pathway 1 (Figure 2). Isomeric structures for the $[MLi^+ - 189]$ ion could also result from pathways similar to those in pathway 1. Alternatively, the cyclophosphane may be eliminated as the neutral species depicted in pathway 2 (Figure 2) to yield the $[MLi^+ - 183]$ ion. A variation on pathway 2 is that the diglyceride-like moiety could be eliminated as a neutral species. In that case, the charged species resulting from the elimination would be a lithiated cyclophosphane with an m/z value of 131. An ion with that mass-to-charge ratio value, although of low abundance, is observed in the spectra in Figure 1B, C, D. Pathways similar to those in Figure 2 (pathways 1 and 2) have been used to rationalize head-group eliminations from sodiated GPC species [27].

Among the more abundant ions in the spectra in Figure 1B, C, D that yield information about the fatty acid substituents are the $[MLi^+ - 59 - R_xCOOH]$ ions, and they may also arise (via pathways 3 and 4, respectively) from the intermediate structure resulting from initial loss of trimethylamine depicted in Figure 2. Losses like those in pathways 3 and 4 could also occur directly from the $[MLi^+]$ ion to yield the $[MLi^+ - R_xCOOH]$ ions observed in the spectra in Figure 1B, C, D. The mechanisms for fatty acid elimination depicted in pathways 3 and 4 (Figure 2) have been used to rationalize elimination of fatty acids from other phospholipid ions [18]. The pathways in Figure 2 are consistent with tandem mass spectra obtained from CAD of the $[MLi^+]$ ions of two deuterated analogs of (14:0/14:0)-GPC. These analogs contained either four deuterium atoms on the methylene moieties of the choline group or nine deuterium atoms on the methyl substituents of the quaternary amine. Table 1 contains the mass-to-charge ratio values and relative abundances of the ions summarized in Figure 2 for native (14:0/14:0)-GPC and for the two deuterated analogs. In each case, the mass-to-charge ratio values for these ions shifted or failed to shift in the manner expected from the pathways in Figure 2 and from the location of the deuterium atoms. This was also true for the mass-to-charge ratio value of the ion thought to represent the lithiated cyclophosphane moiety (Table 1, last column).

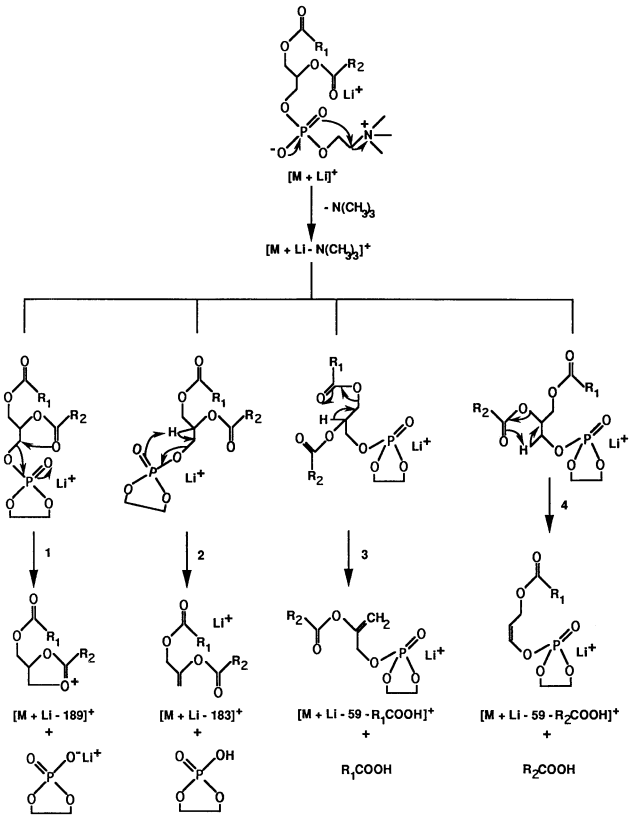

Figure 2. Proposed pathways for generation of five informative ions in the tandem mass spectra of lithiated adducts of glycerophosphocholine lipids. The pathways are proposed to rationalize $[MLi^+ - 59]$ (initial step), $[MLi^+ - 189]$ (pathway 1), $[MLi^+ - 183]$ (pathway 2), $[MLi^+ - 59 - R_1CO_2H]$ (pathway 3), and $[MLi^+ - 59 - R_2CO_2H]$ (pathway 4) ions observed in the tandem mass spectra of GPC-Li^+ adducts.

To determine whether the relative abundances of ions reflecting losses of the fatty acid substituents from lithiated GPC species might indicate the positions of these substituents, two sets of positional isomers of synthetic standard GPC species were examined (Figure 3). The first set was (14:0/16:0)-GPC (Figure 3A) and (16:0.14:0)-GPC. (Figure 3B). CAD of the $[MLi^+]$ ions (m/z 712) of these compounds yielded tandem spectra that contained ions reflecting loss of myristic acid (m/z 484), of the lithium salt of myristate (m/z 478), of palmitic acid (m/z 456), of the lithium salt of palmitate (m/z 450), and of trimethylamine plus either myristic acid (m/z 425) or palmitic acid (m/z 397). Comparison of the relative abundances of the ions at m/z 425

Table 1. Summary of fragment ions reflecting net losses of trimethylamine, of the entire head group, or of trimethylamine plus the fatty acid substituent observed in CAD tandem mass spectra of lithiated species of standard glycerophosphocholine lipids with isotopes of hydrogen at various positions in the head group

			Fragment ions from losses of A through D[a]									
			A		B		C		D		$(C[^{X}H_2])_2PO_4HLi^+$	
No.	GPC species	MLi^+	*m/z*	(ra)	*m/z*	(ra)	*m/z*	(ra)	*m/z*	(ra)	*m/z*	(ra)
(1)	14:0/14:0-GP-$(CH_2)_2N(CH_3)_3$	684	625	(02)	501	(32)	495	(100)	397	(35)	131	(05)
(2)	14:0/14:0-GP-$(CD_2)_2N(CH_3)_3$	688	629	(03)	501	(48)	495	(100)	401	(35)	135	(07)
(3)	14:0/14:0-GP-$(CH_2)_2N(CD_3)_3$	693	625	(02)	501	(34)	495	(100)	397	(21)	131	(06)

[a]Identification of losses A through D: A = $N(C[^{Y}H_3])_3$, B = $HPO_4(C[^{X}H_2])_2N(C[^{Y}H_3])_3$, C = $HPO_4(C[^{X}H_2])_2N(C[^{Y}H_3])_3$, D = A+$RCO_2H$. For compound No. (1), $x = 1$ and $y = 1$. For compound No. (2), $x = 2$ and $y = 1$. For compound No. (3), $x = 1$ and $y = 2$.
CAD tandem spectra were obtained using a collision energy of 35 eV. Identified losses reflect net, not necessarily direct, elimination of the indicated moieties. The abbreviation "ra" denotes relative abundance (in percent). The designation "$(C[^{X}H_2])_2PO_4HLi^+$" denotes a lithiated five-membered cyclophosphane moiety. The proposed structure of the neutral, nonlithiated cyclophosphane moiety is illustrated in the lowermost structural diagram in pathway 2 of Figure 2.

and 397 in Figure 3A, B indicates that the abundance of the ion reflecting loss of trimethylamine plus the sn-1 substituent exceeds that of the ion reflecting loss of trimethylamine plus the sn-2 substituent.

That phenomenon is further illustrated with a second set of positional isomers of GPC standards, (16:0/18:1)-GPC (Figure 3C) and (18:1/16:0)-GPC (Figure 3D). CAD of the $[MLi^+]$ ions (*m/z* 766) of these compounds yields tandem mass spectra that contain ions reflecting losses of palmitic acid (*m/z* 510), of the lithium salt of palmitate (*m/z* 504), of oleic acid (*m/z* 484), of the lithium salt of oleate (*m/z* 478), and of trimethylamine plus either palmitic acid (*m/z* 451) or oleic acid (*m/z* 425). Comparison of the relative abundances of the ions at *m/z* 425 and 451 in Figure 2C, D again indicates that the abundance of the ion reflecting loss of trimethylamine plus the sn-1 substituent exceeds that of the ion reflecting loss of trimethylamine plus the sn-2 substituent. Similar behavior was observed with lithiated adducts of all other asymmetrical standard GPC species that were examined (Table 2).

Because the loss of one fatty acid substituent yields a fragment ion structure that retains the other fatty acid substituent, tandem mass spectrometric scanning for parents of such fragment ions can be used to identify the fatty acid substituents of lithiated GPC species in mixtures. Similar information can be obtained by scanning for parents that undergo neutral losses of fatty acids or their lithium salts with or without loss of trimethylamine. Table 3 summarizes the fragment ions resulting from these losses for parent GPC-Li^+ ions that contain specific fatty acid substituents. Similar tandem mass spectrometric scans monitoring losses of 59 (trimethylamine), 183 (net loss of $[HPO_4(CH_2)_2N(CH_3)_3]$), or 189 (net loss of $[LiPO_4(CH_2)_2N(CH_3)_3]$) can be used to identify parent ions which contain the phosphocholine head-group in lipid mixtures. Although ions reflecting these losses are observed in the tandem mass spectra of all GPC-Li^+ species examined, their relative abundances are affected by the fatty acid substituents. The ratio for the abundance of the $(MLi^+ - 183)$ ion divided by that of the $(MLi^+ - 189)$ ion increases with the degree of unsaturation of the sn-2 substituent and is about 0.5 for (16:0/16:0)-GPC-Li^+ and about 5 for (18:0/20:4)-GPC-Li^+ (Figure 1).

The potential utility of forming lithiated adducts to identify GPC species in tissue phospholipids was examined next. Various GPC species in extracts of phospholipids from rat liver exhibited similar apparent relative abundances when examined by ESI/MS in positive ion mode as either protonated (Figure 4A) or lithiated (Figure 4B) adducts. The ESI/MS profile of lithiated GPC adducts was also similar when phospholipid extracts from liver were compared to NP-HPLC-purified GPC species (not shown). The ESI/MS profile of GPC species contained in phospholipid extracts from rat brain (Figure 4C) differed from that of the GPC species from rat liver (Figure 4B) when the molecules in both extracts were examined as lithiated species. This illustrates that different tissues within the same organism express some common GPC species with different relative abundances, as reflected, for example, by the different relative intensities of the ion at *m/z* 788 in Figure 4B, C. Some GPC species that are prominent components of one tissue are virtually absent from another, as indicated by comparing the abundance of the ion at *m/z* 740 in Figure 4B, C.

That all of the major species visualized in the total positive ion current of the crude rat liver phospholipid extract (Figure 4B) contained the phosphocholine head-group was confirmed by scanning for parents which undergo losses of the head-group or a component of it (Figure 5). Such losses included 183 (Figure 5A), 189 (Figure 5B), and 59 (Figure 5C). The differing apparent relative abundances of various parents in the scans in Figure 5A, B reflect the influence of fatty acid composition on the losses of 183 and 189, as discussed above. The intensity of the ion reflecting loss of trimethylamine (Figure 5C) also varies among different molecular species with a phosphocholine head-group and appears to be especially favored in sphingomyelin (SM) species. This accounts for the appearance of prominent ions at *m/z* 709 (16:0-SM) and *m/z* 737 (18:0-SM) in the spectrum in Figure 5C even though ions with these

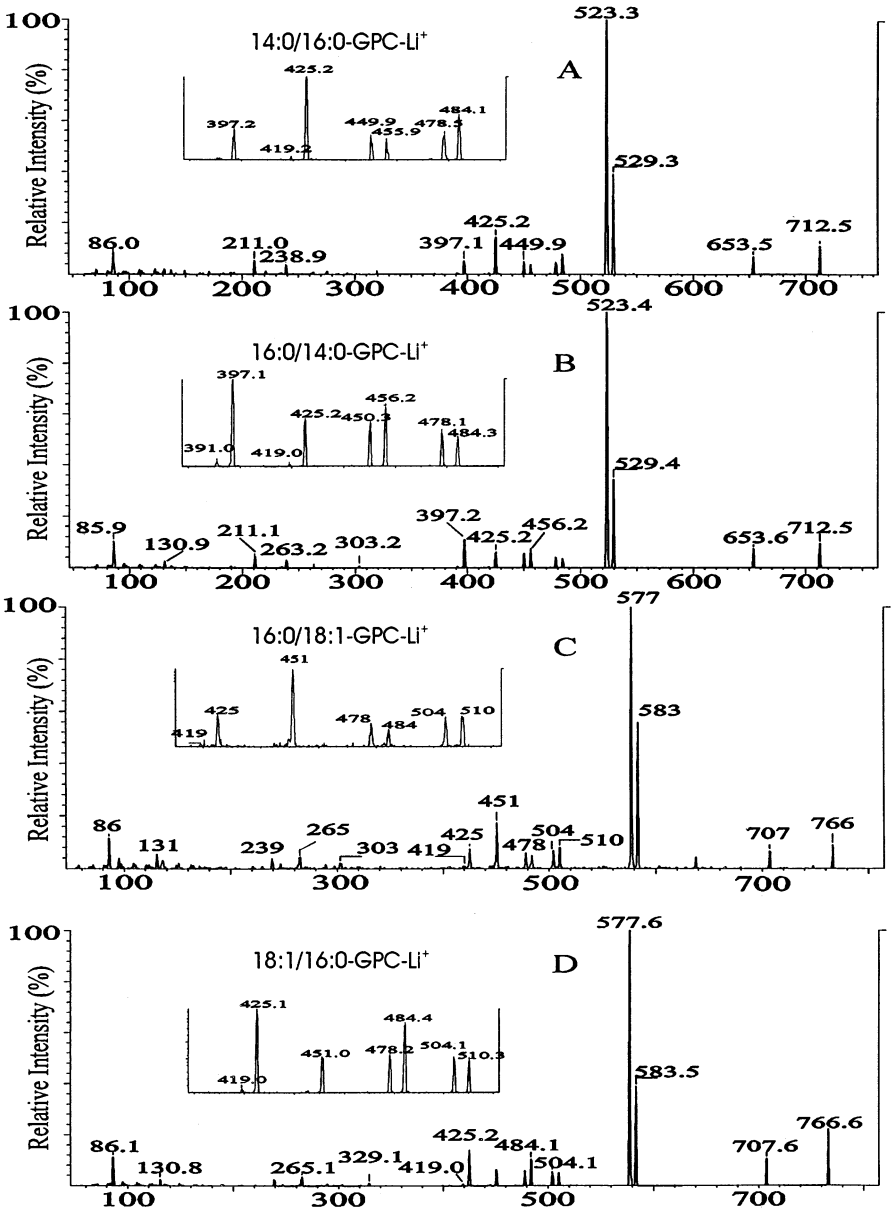

Figure 3. Positive ion ESI tandem mass spectra of lithiated adducts of positional isomers of asymmetrical standard glycerophosphocholine species. Panels are tandem mass spectra obtained from CAD of [MLi$^+$] ions of (14:0/16:0)-GPC (panel A), (16:0/14:0)-GPC (panel B), (16:0/18:1)-GPC (panel C), or (18:1/16:0)-GPC (panel D).

mass-to-charge ratio values are of low abundance in the spectrum in Figure 4B. The combination of the three neutral loss scans identifies both glycerolipid and sphingolipid parents that contain the phosphocholine head-group in tissue phospholipid mixtures.

Figure 6 illustrates that assignment of the fatty acid composition of GPC species in tissue phospholipid mixtures is facilitated by scanning for parents of fragment ions that have lost one fatty acid substituent and retain the other. For example, lithiated GPC species that contain stearate yield a prominent ion at m/z 453 upon CAD (Table 3). This ion reflects neutral loss of the other fatty acid substituent plus trimethylamine (Table 3). As illustrated in Figure 6A, when scanning for parents of m/z 453 is performed with lithiated adducts of rat liver phospholipids, the two most abundant species visualized exhibit mass-to-charge ratio values consistent with (18:0/18:2)-GPC-Li$^+$ (m/z 792) and with (18:0/20:4)-GPC-Li$^+$ (m/z 816), respectively. A similar profile is obtained by scanning for neutral loss of 343 (Figure 1B), which reflects loss of stearic acid plus trimethylamine from the parent ion (Table 3). The possibility that the parent ion at m/z 816 in Figure 6A contains arachidonate (20:4) is supported by linked scanning for parents of m/z 473 (Figure 6C) and for neutral loss of 475 (Figure 6D), both of which reflect arachidonate-contain-

Table 2. Summary of fragment ions observed in CAD tandem mass spectra of lithiated species of standard glycerophosphocholine lipids that reflect the identities and positions of the fatty acid substituents

Standard GPC species	MLi^+ *m/z*	Fragment ions observed on CAD from losses of A through G[a]														Ratio [C(ra)/F(ra)]
		A		B		C		D		E		F		G		
		m/z	(ra)	*m/z*	(ra)	*m/z*	(ra)	*m/z*	(ra)	*m/z*	(ra)	*m/z*	(ra)	*m/z*	(ra)	
14:0/14:0	684	456	(07)	450	(17)	397	(35)	sym		sym		sym		NA		NA
14:0/16:0	712	484	(08)	478	(06)	425	(17)	456	(06)	450	(07)	397	(06)	NA		2.8
16:0/14:0	712	456	(07)	450	(05)	397	(14)	484	(03)	478	(04)	425	(06)	NA		2.3
16:0/16:0	740	484	(13)	478	(11)	425	(33)	sym		sym		sym		NA		NA
16:0/18:2	764	508	(22)	502	(15)	449	(33)	484	(09)	478	(12)	425	(11)	NA		2.5
16:0/18:1	766	510	(11)	504	(09)	451	(22)	484	(06)	478	(07)	425	(09)	NA		2.4
16:0/20:4	788	532	(08)	526	(06)	473	(22)	484	(02)	478	(08)	425	(07)	313	(32)	3.1
18:0/20:4	816	532	(08)	526	(09)	473	(21)	512	(04)	506	(07)	453	(06)	341	(32)	3.5

[a]Identification of losses A through G: A = R_1CO_2H, B = R_1CO_2Li, C = A+$N(CH_3)_3$, D = R_2CO_2H, E = R_2CO_2Li, F = D+$N(CH_3)_3$, G = $LiPO_4(CH_2)_2N(CH_3)_3+R_2{=}C{=}O$.
CAD tandem spectra were obtained using a collision energy of 35 eV. Identified losses reflect net, not necessarily direct, elimination of the indicated moieties. Abbreviations "ra," "sym," and "NA" denote relative abundance (in percent), a symmetrical species, and not applicable, respectively.

ing parents (Table 3). Both scans contain a prominent ion at *m/z* 816, and, in conjunction with the scan in Figure 6A, this indicates that the ion at *m/z* 816 reflects a parent that contains both arachidonate and stearate. Because the neutral loss scans in Figure 5 indicate that the parent at *m/z* 816 also contains a phosphocholine head-group, the parent species can be identified as (18:0/20:4)-GPC-Li^+. This assignment was confirmed by the full-scan tandem mass spectrum produced by CAD of *m/z* 816. This spectrum was identical to that in Figure 1D.

Similarly, the possibility that the parent ion at *m/z* 792 in Figure 6A contains linoleate (18:2) is supported by scanning for parents of *m/z* 449 (Figure 6E), an ion generated from parents that contain linoleate (Table 3). This scan (Figure 6E) contains a prominent ion at *m/z* 792, and, in conjunction with the parent ion scan in Figure 6A and the neutral loss scans in Figure 5, identifies the parent species as (18:0/18:2)-GPC-Li^+. This assignment was confirmed by the full-scan tandem mass spectrum produced by CAD of *m/z* 792 (not shown). Similar scanning for parents of *m/z* 425 (Figure 6F) or neutral loss of 315 (not shown) identifies 16:0-containing parents (Table 3) in the liver phospholipid mixture, the two most abundant of which can be assigned as (16:0/18:2)-GPC-Li^+ (*m/z* 764) and (16:0/20:4)-GPC-Li^+ (*m/z* 788) by comparison of Figure 6F with Figure 6E, C, respectively. These assignments were supported by full-scan tandem mass spectra produced by CAD of *m/z* 764 and *m/z* 788 (not shown).

Such tandem mass spectrometric scans also permit identification of minor components of tissue phospholipid mixtures that may not be readily appreciated from the ESI/MS total ion current profile. For example, the scan in Figure 6F reveals a parent with *m/z* 740 that contains palmitate, although this species is poorly visualized in the total ion current profile of Figure 5B. This ion represents (16:0/16:0)-GPC-Li^+, and, upon CAD and tandem mass spectrometry, this species yields a strong signal on scans that identify palmitate-containing parents because loss of either the sn-1 or sn-2 substituent yields the monitored product ion. Tandem mass spectrometry scanning also facilitates distinction among isobaric components of mixtures. For example,

Table 3. Summary of fragment ions from lithiated glycerophosphocholine molecular species that contain information about the fatty acid substituents

	Lithiated GPC species with the following Rx fatty acid substituents						
	14:0	16:0	18:0	18:1	18:2	20:4	
Are parents of the ions:	397	425	453	451	449	473	from loss of $RyCO_2H+(CH_3)_3N$
	450	478	506	504	502	526	from loss of $RyCO_2Li$
	456	484	512	510	508	532	from loss of $RyCO_2H$
	211	239	267	—	—	—	$RxC{\equiv}O^+$
Undergo neutral losses of:	287	315	343	341	339	363	loss of $RxCO_2H+(CH_3)_3N$
	234	262	290	288	286	310	loss of $RxCO_2Li$
	228	256	284	282	289	304	loss of $RxCO_2H$
	—	—	—	—	—	475	loss of $Rx{=}C{=}O+LiPO_4(CH_2)_2N(CH_3)_3$

Of the two fatty acid substituents in GPC species, one is designated Rx and the other Ry. The specified losses reflect net, not necessarily direct, elimination of the indicated moieties.

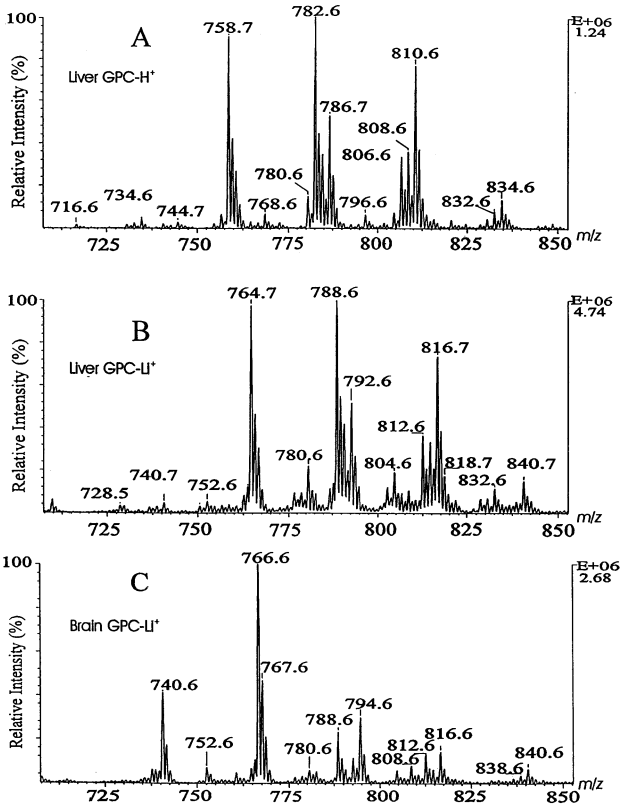

Figure 4. ESI/MS total positive ion current profiles of cationic adducts of glycerophosphocholine species in rat tissue extracts. Panels represent ESI/MS analyses of protonated (panel A) or lithiated (panels B and C) adducts of GPC species in extracts from rat liver (panels A and B) or brain (panel C).

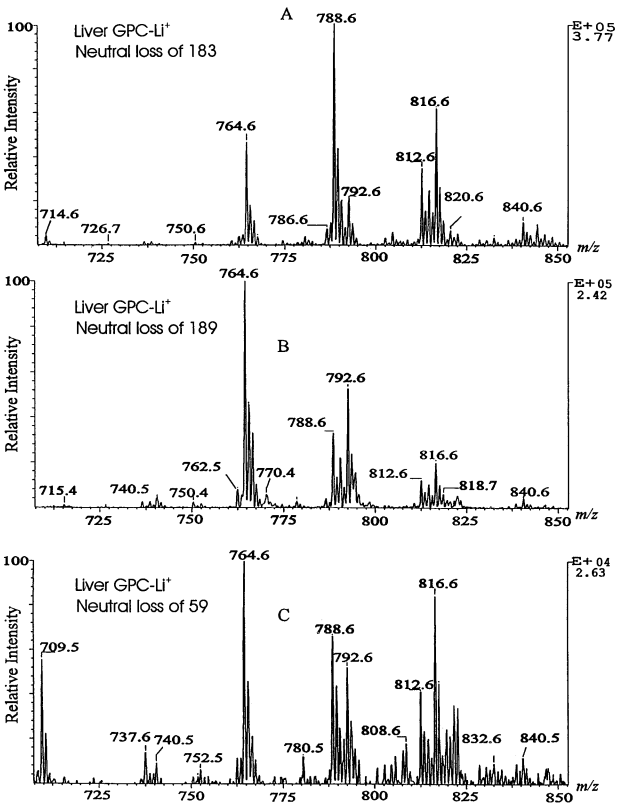

Figure 5. Identification of rat liver phospholipid species that contain a phosphocholine head-group by tandem mass spectrometric scanning for lithiated parents that undergo neutral losses of the head-group or trimethylamine. Positive ion ESI/MS/MS analyses of lithiated adducts of rat liver phospholipids were performed to monitor neutral loss of 183 (panel A), 189 (panel B), or 59 (panel C), reflecting net elimination of $[HPO_4(CH_2)_2N(CH_3)_3]$, $[LiPO_4(CH_2)_2N(CH_3)_3]$, or $[N(CH_3)_3]$, respectively.

the ion at m/z 812 in Figure 4B could represent (18:2/20:4)-PC-Li^+ or (16:0/22:6)-PC-Li^+. The parent ion scan in Figure 6F indicates that this species contains palmitate (16:0), but the scans in Figure 6E, C indicate that the species does not contain either linoleate (18:2) or arachidonate (20:4). This suggests that the species represents (16:0/22:6)-GPC-Li^+. This was confirmed by scanning for parents of m/z 497, which identifies 22:6-containing precursors, and by the full-scan tandem mass spectrum produced by CAD of the parent ion at m/z 812 (not shown). In a similar manner, tandem mass spectrometry scanning can establish that parent ions are composed of isobaric components. For example, scans for parents of m/z 473 (which identifies 20:4-containing precursors), of m/z 499 (which identifies 22:5-containing precursors), and m/z 451 (which identifies 18:1-containing precursors) indicate that the ion at m/z 814 in Figure 4B represents both (18:1/20:4)-PC-Li^+ and of (16:0/22:5)-PC-Li^+.

A summary of the GPC molecular species identified in extracts from rat liver and brain is provided in Table 4, and a summary of fragment ions in the CAD tandem mass spectra of the lithiated adducts of these compounds is provided in Table 5.

Discussion

The ability to analyze tissue phospholipids mixtures directly by ESI/MS/MS has simplified identification of components of such mixtures [26–29]. Such direct analyses circumvent analyte losses incurred in conventional methods of phospholipid analysis, which have involved two sequential HPLC steps, solvolysis, and GC/MS analyses. Although the sensitivity and structural specificity of negative ion ESI/MS/MS is excellent for phospholipid species that readily form negative ions, the presence of a quaternary nitrogen moiety in GPC species favors formation of cationic species, and tandem mass spectra of protonated GPC species contain no abundant ions that identify the fatty acid substituents [18, 20–23, 27].

Our findings indicate that conversion of GPC species to lithiated adducts facilitates their identification by positive ion ESI/MS/MS. Lithiated adducts yield signal similar to that of protonated adducts in terms of absolute intensity and relative abundance among distinct GPC molecular species. Lithiated adducts of GPC species undergo more extensive fragmentation upon CAD

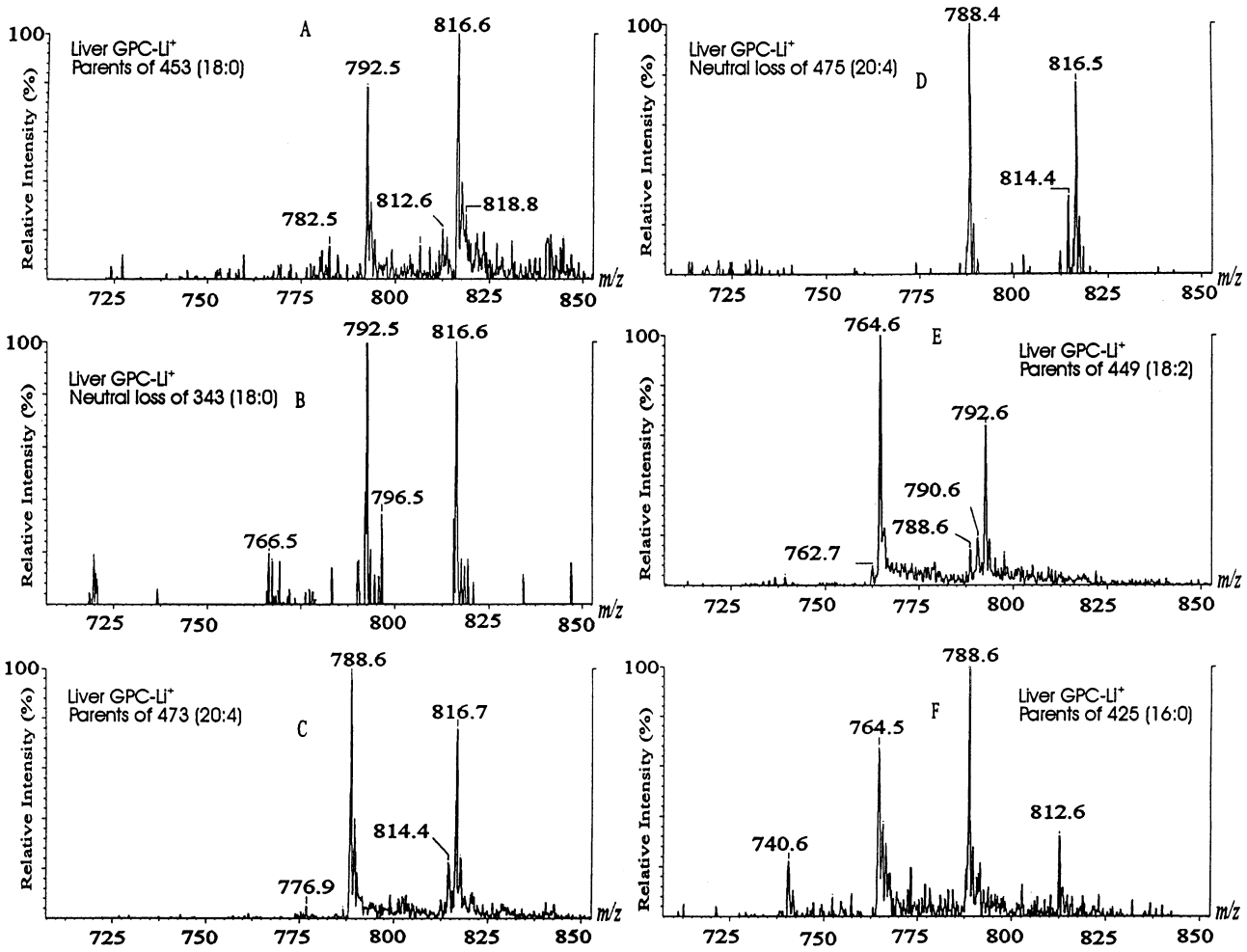

Figure 6. Identification of fatty acid substituents in glycerophosphocholine species in rat liver phospholipids by tandem mass spectrometric scanning for parents of fragment ions that contain specific fatty acid substituents or by scanning for parents that undergo neutral losses reflecting such substituents. Lithiated adducts of phospholipids in a rat liver extract were analyzed by ESI/MS/MS, and scans were performed to identify parents that yielded product ions at m/z 453 (panel A), 473 (panel C), 449 (panel E), or 425 (panel F) to identify parents that contained stearate (panel A), arachidonate (panel C), linoleate (panel E), or palmitate (panel F). Panels B and D are scans that identify parent ions that undergo neutral loss of 343 or 475, respectively. These scans identify stearate- (panel B) or arachidonate-containing (panel D) GPC-Li^+ parents.

than do protonated adducts, and the tandem mass spectra of lithiated adducts include ions reflecting informative losses of the fatty acid substituents and of the phosphocholine head-group. These losses permit the use of tandem mass spectrometry scans to identify GPC species in tissue phospholipid mixtures and their fatty acid substituents. For example, arachidonate-containing parents can be identified either by scanning for parents of the ion at m/z 473, which arises from loss of the other fatty acid substituent plus trimethylamine, or by scanning for parents that undergo neutral loss of 475, reflecting net, though not direct, elimination of $[LiPO_4(CH_2)_2N(CH_3)_3]$ and of arachidonate as a substituted ketene.

Arachidonic acid is metabolized into second messenger substances, including prostaglandins, thromboxanes, and leukotrienes [33]. Arachidonic acid released from tissue phospholipids may also have intrinsic signaling functions, which do not require its conversion to a metabolite [34–40]. Considerable interest has therefore focused on the selective loss of esterified arachidonate from tissue phospholipid species upon stimulation of cells with activating ligands [29, 41, 42], on the transfer of arachidonate among phospholipid headgroup classes and specific intracellular membrane compartments [8, 15–17, 43], and on the role of arachidonate-containing GPC species to serve as precursors of the autacoid Platelet Activating Factor [44]. Facile means for specific identification of arachidonate-containing phospholipid species may be helpful in the further study of such issues. The tandem mass spectrometry scanning methods described here may be

Table 4. Molecular species of glycerophosphocholine observed in rat liver and brain by ESI tandem mass spectrometric analysis of lithiated adducts

MLi^+ *m/z*	Glycerophosphocholine molecular species	Relative intensity	
		Liver	Brain
740	16:0/16:0	0.2	39
764	16:0/18:2	90	6
766	16:0/18:1	10	100
768	16:0/18:0	0	20
788	16:0/20:4	100	25
790	(18:1/18:2)+(16:0/20:3)	28	6
792	18:0/18:2	32	10
794	18:0/18:1	1	35
812	16:0/22:6	22	12
814	(16:0/22:5)+(18:1/20:4)	15	6
816	18:0/20:4	68	14

GPC species in extracts from rat liver and brain were analyzed as lithiated adducts by positive ion ESI/MS and ESI/MS/MS. The tabulated relative intensities of the parent ions were determined from the ESI/MS profile. The identities of the indicated species were determined from their tandem mass spectra.

useful in this regard and serve to distinguish arachidonate-containing GPC species from isobaric GPC species that occur in tissue phospholipid mixtures (e.g., 18:1/20:4-GPC vs. 16:0/22:5-GPC or 18:0/20:4-GPC vs. 16:0/22:4-GPC).

Because of the importance of identifying GPC species in biological mixtures, several successful methods have been developed for this purpose [18, 27, 45–48]. Negative ion FAB/MS/MS performed with anions generated from GPC species in the ion source (by loss of choline, loss of the quaternary amine moiety, or loss of a methyl group from that moiety) permits structural identification of GPC species [18]. Structural identification has also been achieved by negative ion ESI/MS/MS analyses of chloride adducts of GPC species [27]. HPLC/ESI/MS has also been used to examine GPC species in biological extracts, and this approach permits quantitative analyses [45, 46]. Informative fragmentation in positive ion mode has also been demonstrated after thermospray ionization of intact GPC molecules [47] and after chemical ionization of diglyceride moieties derived from GPC species [48]. Depending on available instrumentation and analytic objectives, any of the above approaches can yield useful information about GPC species in biological mixtures. We believe that positive ion ESI/MS/MS analysis of lithiated adducts of GPC species represents a potentially useful complement to the approaches described above. Our findings indicate that positive ion ESI/MS/MS analysis of GPC species as lithiated adducts offers advantages over analysis of protonated adducts and that this approach can distinguish many GPC species in biological mixtures even under circumstances in which the available instrument configuration precludes prior LC separation or in which such separation is impractical for other reasons.

Table 5. Summary of fragment ions observed in CAD tandem mass spectra of lithiated species of glycerophosphocholine from rat liver and brain

GPC species	MLi^+	Fragment ions observed on CAD											
		From losses of A through J[a]										From acylium ions	
		A	B	C	D	E	F	G	H	I	J	R_1CO^+	R_2CO^+
16:0/16:0	740	681	557	551	484	478	484	478	425	425	—	239	239
16:0/18:2	764	705	581	575	508	502	484	478	449	425	—	239	263
16:0/18:1	766	707	583	577	510	504	484	478	451	425	—	239	265
16:0/20:4	768	729	605	599	532	526	484	478	473	425	313	239	—
18:1/18:2	790	731	607	601	508	502	512	506	449	453	—	—	—
16:0/20:3	790	731	607	601	534	528	484	478	475	425	313	239	—
18:0/18:2	792	733	609	603	508	502	512	506	449	453	—	267	263
18:0/18:1	794	735	611	605	510	504	512	506	451	453	—	—	—
16:0/22:5	814	755	631	625	558	552	484	478	499	425	—	239	—
18:1/20:4	814	755	631	625	532	526	510	504	473	451	339	—	—
18:0/20:4	816	757	633	627	532	526	512	506	473	453	341	—	—

[a]Identification of losses A through J: A = $N(CH_3)_3$, B = $HPO_4(CH_2)_2N(CH_3)_3$, C = $LiPO_4(CH_2)_2N(CH_3)_3$, D = R_1CO_2H, E = R_1CO_2Li, F = R_2CO_2H, G = R_2CO_2Li, H = A+D, I = A+F, J = C+R_2 = C = O.
The identified losses reflect net, not necessarily direct, elimination of the indicated moieties.

Acknowledgments

This work was supported by grants from the United States Public Health service (NIH R37-DK-34388, P41-RR-00954, and S10-RR-11260) and by the Washington University Diabetes Research and Training Center (P60-DK-20579). Excellent technical assistance was provided by Dr. Mary Wohltmann and excellent secretarial services by Anita Zinna.

References

1. Chapman, D.; Wallich, D. F. H. *Biological Membranes*; Academic: New York, 1989; p 71.
2. Gross, R. W. *Biochemistry* **1984,** *23*, 158–165.
3. Gross, R. W. *Biochemistry* **1985,** *24*, 1662–1668.
4. Ramanadham, S.; Bohrer, A.; Mueller, M.; Jett, P.; Gross, R. W.; Turk, J. *Biochemistry* **1993,** *32*, 5339–5351.
5. Ramanadham, S.; Bohrer, A.; Gross, R. W.; Turk, J. *Biochemistry* **1993,** *32*, 13499–13509.
6. Glaser, P. R.; Gross, R. W. *Biochemistry* **1994,** *33*, 5805–5812.
7. Glaser, P. R.; Gross, R. W. *Biochemistry* **1995,** *34*, 12193–12203.
8. Surette, M. E.; Winkler, J. D.; Fonteh, A. N.; Chilton, F. H. *Biochemistry* **1996,** *35*, 9187–9196.
9. Prescott, S. M. *J. Biol. Chem.* **1997,** *272*, 15043.
10. Rhee, S. G.; Bae, Y. S. *J. Biol. Chem.* **1997,** *272*, 15045–15048.
11. Exton, J. H. *J. Biol. Chem.* **1997,** *272*, 15579–15583.
12. Balsinde, J.; Dennis, E. M. *J. Biol. Chem.* **1997,** *272*, 16069–16072.
13. Leslie, C. C. *J. Biol. Chem.* **1997,** *272*, 16709–16712.
14. Stafforini, D. M.; McIntyre, T. M.; Zimmerman, G. A.; Prescott, S. M. *J. Biol. Chem.* **1997,** *272*, 17895–17898.
15. Chilton, F. H.; Murphy, R. C. *J. Biol. Chem.* **1986,** *261*, 7771–7777.
16. Balsinde, J.; Bianco, I. D.; Ackerman, E. J.; Dennis, E. A. *Proc. Natl. Acad. Sci.* **1995,** *92*, 8527–8531.
17. Balsinde, J.; Dennis, E. A. *J. Biol. Chem.* **1997,** *272*, 16069–16072.
18. Murphy, R. C.; Harrison, K. A. *Mass Spectrom Rev.* **1994,** *13*, 57–76.
19. Patton, G. M.; Fasulo, J. M.; Robins, S. J. *J. Lipid Res.* **1982,** *23*, 190–196.
20. Jensen, N. J.; Gross, M. L. *Mass Spectrom Rev.* **1988,** *7*, 41–49.
21. Kayganich, K.; Murphy, R. C. *J. Am. Soc. Mass Spectrom.* **1991,** *2*, 45–54.
22. Jensen, N. J.; Tomer, K. B.; Gross, M. L. *Lipids* **1987,** *22*, 480–489.
23. Haroldsen, P. E.; Gaskell, S. J. *Biomed. Environ. Mass Spectrom.* **1989,** *18*, 439–450.
24. Cole, M. J.; Encke, C. G. *Anal. Chem.* **1991,** *63*, 1032–1040.
25. Heller, D. N.; Murphy, C. M.; Cotter, R. J.; Fenselau, C.; Uy, O. M. *Anal. Chem.* **1988,** *60*, 2787–2791.
26. Han, X.; Gross, R. W. *Proc. Natl. Acad. Sci.* **1994,** *91*, 10635–10639.
27. Han, X.; Gross, R. W. *J. Am. Soc. Mass Spectrom.* **1995,** *6*, 1202–1210.
28. Han, X.; Gross, R. W. *J. Am. Chem. Soc.* **1996,** *118*, 451–457.
29. Han, X.; Gubitosi-Klug, R. A.; Collins, B. J.; Gross, R. W. *Biochemistry* **1996,** *35*, 5822–5832.
30. Huang, Z. H.; Cage, D. A.; Sweeley, C. C. *J. Am. Soc. Mass Spectrom.* **1992,** *3*, 71–78.
31. Li, C.; Yergey, J. A. *J. Mass Spectrom.* **1997,** *32*, 314–322.
32. Bligh, E. G.; Dyer, W. J. *Can. J. Biochem. Physiol.* **1959,** *37*, 911–917.
33. Needleman, P.; Turk, J.; Jakschik, B.; Morrison, A.; Lefkowith, *J. Annu. Rev. Biochem.* **1986,** *55*, 69–102.
34. Meeves, H. *Progr. Neurobiol.* **1994,** *43*, 175–176.
35. Shuttleworth, T. J. *J. Biol. Chem.* **1996,** *271*, 21720–21725.
36. Sauvadet, A.; Rohm, R.; Pecker, F.; Pavoine, C. *J. Biol. Chem.* **1997,** *272*, 12347–12445.
37. Wolf, B.; Turk, J.; Sherman, W.; McDaniel, M. L. *J. Biol. Chem.* **1986,** *261*, 3501–3510.
38. Wolf, B. A.; Pasquale, S. M.; Turk, J. *Biochemistry* **1991,** *30*, 6372–6379.
39. Ramanadham, S.; Gross, R. W.; Turk, J. *Biochem. Biophys. Res. Commun.* **1992,** *184*, 647–653.
40. Ramanadham, S.; Gross, R.; Han, X.; Turk, J. *Biochemistry* **1993,** *32*, 337–346.
41. Purdon, A. D.; Patelunas, D.; Smith, J. B. *Lipids* **1987,** *22*, 116–120.
42. Ford, D. A.; Gross, R. W. *Proc. Natl. Acad. Sci.* **1989,** *86*, 3479–3483.
43. DaTorre, S. D.; Creer, M. H. *J. Lipid Res.* **1991,** *32*, 1159–1172.
44. Ramesha, C. S.; Pickett, W. C. *J. Lipid Res.* **1987,** *28*, 326–331.
45. Ma, Y.-C.; Kim, H.-Y. *Anal. Biochem.* **1995,** *226*, 293–301.
46. Kim, H.-Y.; Wang, T.-C. L.; Ma, Y. C. *Anal. Chem.* **1994,** *66*, 3977–3982.
47. Kim, H.-Y.; Salem, N. *Anal. Chem.* **1986,** *58*, 9–14.
48. Myher, J. J.; Kuskis, A. *Can. J. Biochem.* **1982,** *60*, 638–650.